

KINETIC AND THERMODYNAMIC STUDY OF CHLOROBENZENE ADSORPTION FROM AQUEOUS SOLUTIONS ONTO GRANULAR ACTIVATED CARBON

E.A. CEPEDA, U. IRIARTE and I. SIERRA

Dto. de Ing. Química, Facultad de Farmacia, Universidad del País Vasco, Paseo de la Universidad 7, 01006 Vitoria-Gasteiz, Alava, Spain. E-mail: emilio.cepeda@ehu.es

Abstract— The adsorption of chlorobenzene (CB) from aqueous solutions using granular activated carbon (GAC) of different particle sizes was studied at temperatures from 283 to 303 K. Experimental kinetic values were fitted to a hyperbolic expression, which corresponds to the pseudo-second-order kinetic model. The model predictions are satisfactory in the whole range of particle sizes. Adsorption was found to be governed by intraparticle diffusion. For the adsorption system studied, mass transfer resistance becomes low enough at particle sizes below 1.68 mm to allow an adequate intraparticle transport of solute to the adsorption sites on sorbent surface. Isotherm data were fitted to Langmuir, Freundlich and Redlich-Peterson models. The equilibrium uptake capacity increased with temperature, indicating the endothermic nature of the process. The apparent isosteric heat of adsorption was determined by means of the Clausius–Clapeyron equation being in the 88-288 kJ/mol range.

Keywords— Chlorobenzene, adsorption, activated carbon, kinetics.

I. INTRODUCTION

Chlorobenzene (CB) belongs to a group of ordinary contaminants of water. It can be found in the effluents of many industries such as dyestuff, pesticides and rubber industries in which CB is commonly used solvent. It causes an unpleasant taste and odor, even at low concentration (Environment Protection Agency, 1985) and as other chlorinated benzenes it has carcinogenic effects in humans (Chowdhury and Viraraghavan, 2009), so that in Spain guidelines on maximum allowable concentrations in drinking water are in the order of parts per billion (Real Decreto, 2003)

Adsorbents such as activated carbon (AC) are widely used for the removal of aromatic compounds from aqueous effluents in drinking water production, as well as in the tertiary treatment of wastewater plants (Zhu *et al.*, 2011). Several cheaper adsorbents such as fly ash, silica gel and clay materials have also been applied for organic compound removal (Ahmed and Ram, 1992). Although some studies illustrate the important need of clay materials treated by chemical or physical processes as adsorbents for the removal of organic pollutants and pesticides from water (van den Heuvel and van Noort, 2004; Yapar *et al.*, 2005), in general terms, it has been reported that the uptake capacity of activated carbon is effective for hydrophobic pollutants and poorly water soluble compounds as chlorobenzene (Croue *et al.*, 1999). The high adsorption capacities of activated car-

bons are usually related to their high surface area, pore volume, and porosity (Tsai *et al.*, 2001).

Granular activated carbon (GAC) is being used as an alternative to powdered activated carbon because its use in beds permits high adsorptive capacity and the process control, allowing the filling of the column or the regeneration of exhausted activated carbon. Moreover, GAC has excellent adsorption capacity for many undesirable substances, specially odorous compounds or organic compounds frequently present before finished water as chlorinated benzenes. The adsorption of chlorinated benzenes in liquid phase has been scarcely studied in the literature, due to the difficulty of its analysis and its volatility (Wang and Lee, 1998). It is well known that the adsorption of these hydrocarbons takes place in monolayer when activated carbon is used, whereas it occurs as multilayer when resins are used (Gusler *et al.*, 1993). In a recent article, the adsorption of chlorobenzene with powdered activated carbon was studied at 25 °C considering the influence of two experimental parameters, initial CB concentration and AC dose (Lin *et al.*, 2012). Data for aqueous CB adsorption in GAC analyzing the influence of particle size were not found in the open literature.

The objective of this work was to study the adsorption kinetics, equilibrium and thermodynamics of chlorobenzene in aqueous solutions onto activated carbon of various particle sizes. The influence of adsorption temperature is a relevant issue, since adsorption temperatures may significantly vary depending on the source of wastewater, so the study was made at various temperatures and the isosteric heat of adsorption was also determined.

II. METHODS

A. Materials

Activated carbon manufactured from lignite by DARCO® (Sigma-Aldrich) was used in this study. Particle size varied in the range of 0.250 to 1.68 mm. Activated carbon was previously washed with distilled water, dried in oven at 105 °C for 24 hours and then stored in a desiccator. Textural properties were determined by N₂ adsorption-desorption at 77 K. The measured values of Brunauer-Emmett-Teller (BET) surface area and pore volume were 600 m²/g and 0.95 cm³/g, respectively. Due to the low water solubility of chlorobenzene (analytical grade, purity > 99%, UCB), stock solutions were prepared in acetonitrile. Working solutions were prepared by dilution of the stock solution. The quantification of chlorobenzene was carried out by gas chromatography with a flame ionization detector (FID).

Table 1. Kinetic parameters of best fit for hyperbolic and intraparticle diffusion models.

| | Hyperbolic kinetic model | | | Intraparticle diffusion model | | |
|---|--------------------------|---|--------------------|---|----------------------------|--------------------|
| | $K \text{ min}^{-1}$ | $q_m \text{ g}_{\text{CB}}/\text{g}_{\text{GAC}}$ | $APE \text{ (\%)}$ | $k_d \text{ mg}_{\text{CB}}/(\text{g}_{\text{GAC}} \cdot \text{s}^{0.5})$ | $D_s \text{ m}^2/\text{s}$ | $APE \text{ (\%)}$ |
| $d_p, \text{ mm}$ | | | | | | |
| 0.25-0.35 | 0.154 | 0.0275 | 3.26 | 0.400 | $4.89 \cdot 10^{-7}$ | 3.68 |
| 0.50-0.71 | 0.0479 | 0.0299 | 5.01 | 0.503 | $3.29 \cdot 10^{-6}$ | 5.82 |
| 0.86-1.68 | 0.0236 | 0.0321 | 9.32 | 0.465 | $1.48 \cdot 10^{-5}$ | 10.4 |
| $C_0, \text{ g}_{\text{CB}}/\text{l}$ | | | | | | |
| 0.42 | 0.0944 | 0.0310 | 2.32 | 0.607 | $1.84 \cdot 10^{-6}$ | 4.63 |
| 0.36 | 0.0699 | 0.0320 | 3.11 | 0.529 | $1.39 \cdot 10^{-6}$ | 6.28 |
| 0.23 | 0.0483 | 0.0241 | 6.24 | 0.426 | $1.66 \cdot 10^{-6}$ | 2.00 |
| Mass ratio, $\text{mg}_{\text{CB}}/\text{g}_{\text{GAC}}$ | | | | | | |
| 0.106 | 0.0525 | 0.0309 | 7.60 | 0.671 | $5.24 \cdot 10^{-6}$ | 5.33 |
| 0.053 | 0.0539 | 0.0337 | 2.18 | 0.607 | $3.44 \cdot 10^{-6}$ | 2.71 |
| 0.035 | 0.0867 | 0.0282 | 1.59 | 0.465 | $2.75 \cdot 10^{-6}$ | 4.62 |
| Mean value | | | 4.51 | | | 5.05 |

Chlorobenzene was previously extracted by liquid-liquid extraction with n-pentane. Method standard deviation was below 10 %.

B. Equilibrium and kinetic studies

The equilibrium and kinetic experiments were carried out by shaking batch technique. Activated carbon (dry basis) was weighted and put into glass flasks. For equilibrium experiments, 100 cm³ of aqueous solutions of different initial solute concentration were added and placed in a stirred thermostatic bath (± 0.10 °C). Samples were kept at different temperatures, in the range of 283 to 303 K. After the desired time of treatment, samples were filtered to remove the adsorbent.

Kinetic experiments were carried out using the same procedure; using 250 cm³ of solutions of initial concentrations in the range of 0.23 to 0.42 mg/l at 293 K. Maximum contact time was 120 min in every run. Aqueous solutions were analyzed at different contact times, and the concentration of CB on the adsorbent was calculated based on mass balance:

$$q_t = \frac{V(C_0 - C_t)}{m} \quad (1)$$

where V is the volume of the solution, m is the mass of GAC used (g), and q_t (g_{CB}/g_{GAC}) and C_t (g_{CB}/l) are the concentrations of CB on the adsorbent and in the liquid phase at a time t (min), respectively.

III. RESULTS AND DISCUSSION

A. Adsorption kinetics

There are several kinds of models to describe the adsorption mechanisms and kinetics. A hyperbolic equation, previously used in the literature, was tested (Cotoruelo *et al.*, 2009; Cotoruelo *et al.*, 2010). This hyperbolic expression is a simplification of the pseudo-second-order kinetic equation related to the available sites on the adsorbent surface (Liu, 2008). Experimental data were fitted by nonlinear regression to the following expression:

$$q_t = \frac{kq_m t}{1 + kt} \quad (2)$$

where k is an empirical parameter related to the kinetic curve shape (min⁻¹), and q_m (g_{CB}/g_{GAC}) represents the maximum (asymptotic) q_t value under the experimental

conditions used. Consequently, if contact time is high enough, q_t tends to q_m .

The values of the kinetic parameters of best fit are listed in Table 1. The goodness of fit between the experimental and predicted values was determined by means of the average percentage errors (APE):

$$APE = \frac{\sum_{i=1}^n (q_{e,\text{exp}} - q_{e,\text{predic}}) / q_{e,\text{exp}}}{N} \cdot 100 \quad (3)$$

where N is the number of cases.

Fig. 1 displays the effect of adsorbent particle size on the adsorption time profile. The experimental results (points) and hyperbolic model results (lines) are shown. It is observed that model predictions are satisfactory in the whole range of particle sizes.

The first adsorption stage corresponds to the surface coverage of the largest pores and most active sites. The second stage, with a lower adsorption rate, is related to the coverage of narrow mesopores and micropores. It is evident that an increase in particle size leads to a decrease in the adsorption rate. This is attributed to the greater accessibility to pores and higher surface area per unit weight of the adsorbent, in the case of the small particles.

Solid-liquid adsorption processes on porous materials can be described by consecutive steps involving (i) the mass transfer of the adsorbate from the liquid bulk phase towards the surface of the solid particle across the boundary layer, (ii) the internal diffusion within the particle, and (iii) the adsorption on particle surface. The mass transport resistance inside the solid is usually much more important than that corresponding to the external fluid film on solid particle and the external resistance becomes negligible under suitable shaking conditions.

So, the possibility of intraparticle diffusion to control the kinetics of adsorption was tested using the Eq. (4).

$$q_t = k_d \cdot t^{0.5} + C_i \quad (4)$$

where k_d is the intraparticle diffusion constant and C_i is a constant (i.e. intercept of the line) that is directly pro-

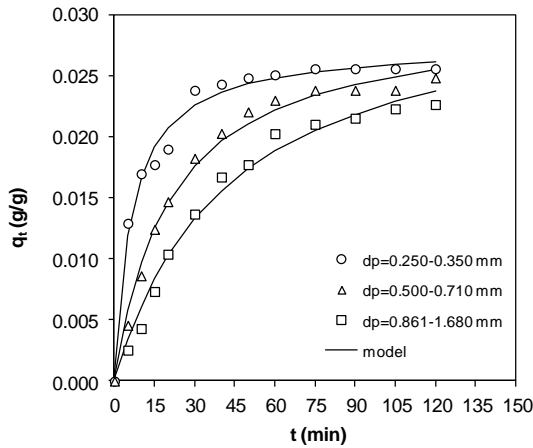


Fig. 1. CB adsorption profile for different adsorbent particle sizes. $m = 1.5 \text{ g}_{\text{GAC}}$, $C_0 = 0.2750 \text{ g/l}$.

portional to the boundary layer thickness. From the intraparticle homogeneous diffusion model, diffusivity values can be estimated as described by Eq. (5).

$$k_d = 6q_e \left(\frac{D_s}{\pi R^2} \right)^{(1/2)} \quad (5)$$

where R is the adsorbent particle radius, q_e is the equilibrium concentration of CB on the adsorbent surface, and D_s is the intraparticle diffusivity.

The effect of particle size, initial concentration of adsorbate and sorbent mass are illustrated in Fig. 2. The intraparticle diffusion is the rate controlling factor, since the uptake of the sorbate varies with the square root of time and two or more steps occur (Walker *et al.*, 2003). Such type of plot presents a multilinearity. The first stage is usually the sharpest and is related to the external surface sorption or instantaneous sorption stage. Its contribution to total mass transfer mechanism can be measured by the value of the intercept with the abscissa axis.

The second portion is the gradual sorption stage, where intraparticle diffusion is rate-controlling. The fact that the plots are not completely linear and do not pass through the origin, indicates that intraparticle diffusion is not the only mechanism involved.

The third portion of the curve is the final equilibrium stage where intraparticle diffusion slows down due to the reduction in the adsorbate concentration in the solution. The fact that the plots are not completely linear and do not pass through the origin, indicates that intraparticle diffusion is not the only mechanism involved.

The linearity of the plots of q_t versus $t^{0.5}$ (Fig. 2) evidences that intraparticle diffusion plays a significant role in the uptake of CB. Measured regression coefficients are larger than 0.955. Values of intraparticle diffusivity are summarized in Table 1.

The intraparticle diffusion coefficient (k_d) remains almost constant with an average value of $0.456 \pm 0.042 \text{ mg}_{\text{CB}}/(\text{g}_{\text{GAC}} \text{ s}^{0.5})$ for every particle size tested (Fig. 2.a). This suggests that for the adsorption system studied at

particle sizes below 1.68 mm mass transfer resistance becomes low enough to allow an adequate intraparticle transport of solute to the adsorption sites on the surface of the sorbent.

Fig. 2.b depicts the favorable effect of the initial concentration of CB on adsorption kinetics. Intraparticle diffusion coefficient values slightly increase with CB initial concentration, which can be attributed to the higher driving force for mass transfer. Measured average value for k_d was $0.521 \pm 0.074 \text{ mg}_{\text{CB}}/(\text{g}_{\text{GAC}} \text{ s}^{0.5})$.

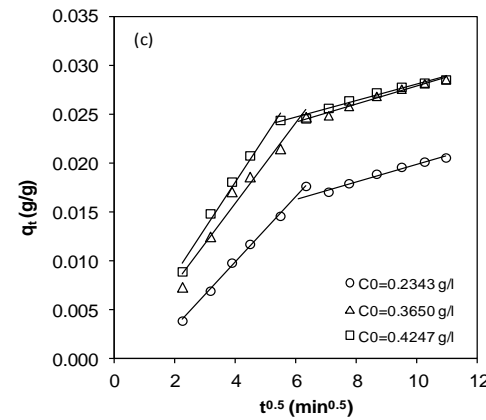
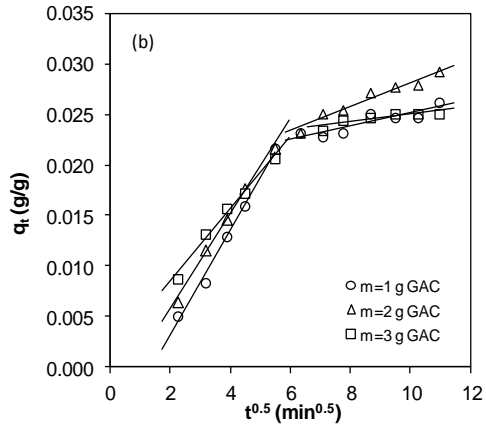
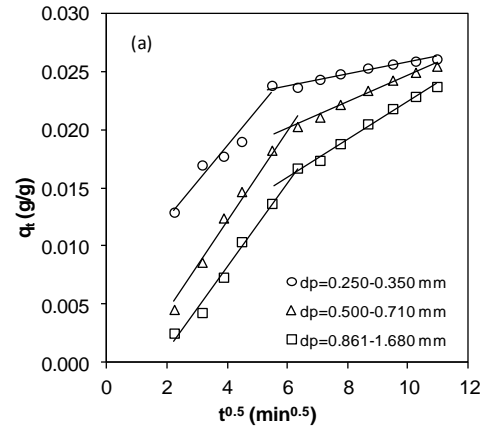


Fig. 2. Intraparticle diffusion model for different adsorption conditions. a) Particle size, $m = 1.5 \text{ g}_{\text{GAC}}$, $C_0 = 0.27 \text{ g/l}$; b) Initial CB concentration, $m = 2.0 \text{ g}_{\text{GAC}}$, $d_p = 0.35\text{-}0.50 \text{ mm}$ and

c) Adsorbent mass. Eq. 4 fits: $C_0 = 0.27 \text{ g/l}$, $d_p = 0.50\text{-}0.71 \text{ mm}$.

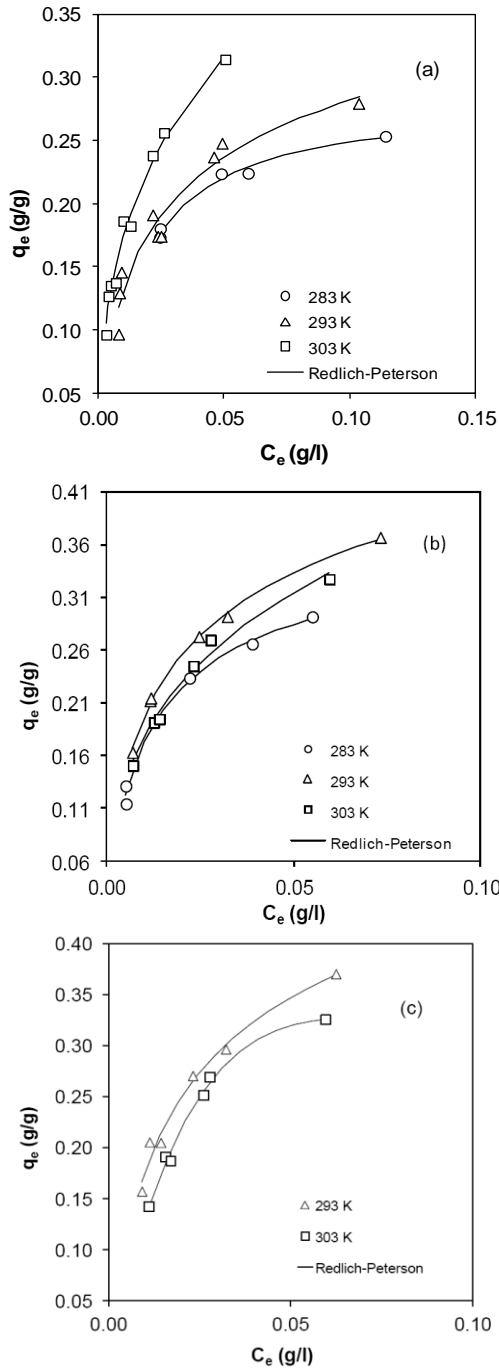


Fig. 3. Experimental results of adsorption isotherms (points) and those calculated with Redlich-Peterson model for different temperatures and adsorbent particle sizes. a) 0.861-1.680 mm; b) 0.5 – 0.71 mm; c) 0.250-0.355 mm.

From results depicted in Fig. 2.c it is observed that when sorbent to solute mass ratio decreases, at constant solute concentration, the intraparticle diffusivity coefficient significantly increases. Data summarized in Table 1 reveal a 44 % increase from 0.465 to 0.671 $\text{mg}_{\text{GCB}}/(\text{g}_{\text{AC}} \text{ s}^{0.5})$. C_i values were in all cases close to zero, except for the lowest adsorbent dose (Fig. 2c), revealing the higher contribution under these conditions of

other sorption mechanisms such as film diffusion or adsorption onto available sites.

B. Adsorption equilibrium

The equilibrium concentrations of chlorobenzene on the adsorbent surface ($q_e, \text{g}_{\text{CB}}/\text{g}_{\text{GAC}}$) were obtained after one week of contact time. Previous experiments confirmed the achievement of equilibrium. Concentration was determined by mass balance as given by Eq. (1).

Figure 3 shows the experimental results of the adsorption of CB in aqueous solution for different particle sizes. It observed that all isotherms are concave with respect to the axis of abscissas; that is to say, as the concentration of the adsorbate in the liquid phase is increased, the concentration on the solid phase increases more slowly. The adsorption system does not reach saturation since the initial solute concentration is limited by CB solubility (water solubility 0.488 g/l) which prevents the preparation of more concentrated working solutions.

Adsorption capacity is significantly increased with temperature of solution indicating the process to be endothermic in nature, which is consistent with studies in the literature for similar adsorption systems (Iriarte-Velasco *et al.*, 2011). An increase in temperature improves the diffusivity of the molecules and, therefore, their access to the pores of the adsorbent is favored.

Figure 3a shows that CB is strongly adsorbed onto GAC at 303 K; for example, for the highest particle size used, a solution containing only 5 mg/l CB produces an equilibrium loading of 135 mg CB per gram of GAC. These values are well above those measured for CB by other adsorbents, such as montmorillonite rich bentonites (Sennour *et al.*, 2009) which yielded uptake capacities in the range of 5.8 to 44.4 mg/g.

Figure 3 also evidences that at low temperatures the uptake capacity of the activated carbon increases as particle size decreases. However, at the smallest particle size, the adsorption isotherms get closer; that is, the influence of temperature is attenuated. Experimental data were fitted to the well-known Langmuir, Freundlich and Redlich-Peterson (Redlich and Peterson, 1959) models, Eqs. 6 to 8, respectively

$$q_e = \frac{q_{ml} k_L C_e}{1 + k_L C_e} \tag{6}$$

$$q_e = k_f C_e^n \tag{7}$$

$$q_e = \frac{AC_e}{1 + BC_e^\beta} \tag{8}$$

where q_e is the amount adsorbed in the equilibrium per unit mass of the adsorbent ($\text{g}_{\text{CB}}/\text{g}_{\text{GAC}}$) and C_e is the solute concentration in solution at equilibrium ($\text{g}_{\text{CB}}/\text{L}$). In Langmuir equation q_{mL} is the monolayer capacity ($\text{g}_{\text{CB}}/\text{g}_{\text{GAC}}$) and k_L is the adsorption coefficient ($\text{L}/\text{g}_{\text{GCB}}$), related to the adsorption energy. Parameters n and k_f ($\text{L}^n \text{g}_{\text{CB}}^{n-1} \text{g}_{\text{GAC}}^{-1}$) are constants. When the value of k_f increases, the capacity of adsorption of the adsorbent for a

certain solute increases. Values in the range $0 < n < 1$ represent favourable adsorption conditions. In Redlich-Peterson equation A is the Redlich-Peterson isotherm

constant (L/g_{CB}), B is another constant (L/g_{CB}) $^\beta$, and β is the Redlich-Peterson exponent, which usually lies between 0 and 1.

Table 2. Parameters of best fit for Langmuir, Freundlich and Redlich-Peterson.

| d_p (mm) | Langmuir | | | | Freundlich | | | Redlich-Peterson | | | |
|-------------------|----------|--------------|------------------------------|------------|--------------------------------|-------|------------|---------------------|-----------------------------|---------|------------|
| | T K | k_L L/g | q_{mL} g_{CB}/g_{GAC} | APE (%) | k_F $L^n g_{GAC}^{(n-1)}$ | n | APE (%) | A g_{GAC}^{-1} | B L^β/g_{CB}^β | β | APE (%) |
| 0.861-1.68 | 303 | 102.1 | 0.363 | 7.96 | 1.0782 | 0.398 | 5.56 | 151.7 | 176.1 | 0.6800 | 5.12 |
| | 293 | 69.45 | 0.310 | 8.45 | 0.6235 | 0.330 | 8.46 | 35.31 | 78.84 | 0.8352 | 8.19 |
| | 283 | 66.08 | 0.287 | 1.59 | 0.4275 | 0.232 | 2.54 | 17.66 | 64.10 | 1.022 | 1.62 |
| 0.500-0.71 | 303 | 74.46 | 0.391 | 3.27 | 0.9159 | 0.361 | 2.99 | 147.5 | 179.9 | 0.6899 | 2.48 |
| | 293 | 88.99 | 0.405 | 3.01 | 0.8463 | 0.318 | 3.10 | 64.89 | 104.8 | 0.8246 | 1.23 |
| | 283 | 109.2 | 0.329 | 4.11 | 0.8499 | 0.364 | 5.32 | 43.22 | 101.1 | 0.9056 | 3.67 |
| 0.25-0.355 | 303 | 44.82 | 0.458 | 3.98 | 1.1548 | 0.434 | 6.73 | 14.5 | 114.0 | 1.5023 | 2.26 |
| | 293 | 60.17 | 0.463 | 3.78 | 1.1208 | 0.392 | 5.31 | 34.70 | 56.50 | 0.8841 | 3.81 |
| Mean value | | | | 4.52 | | | 5.00 | | | | 3.55 |

Table 3. Apparent isosteric heats of adsorption, calculated for different temperature ranges. $d_p=0.5 - 0.71$ mm.

| 283-293 K | | 293-303 K | |
|-----------------------------|------------------------|-----------------------------|------------------------|
| q (g_{CB}/g_{GAC}) | ΔH (kJ/mol) | q (g_{CB}/g_{GAC}) | ΔH (kJ/mol) |
| 0.05 | 87.57 | 0.05 | 287.62 |
| 0.06 | 82.55 | 0.06 | 280.51 |
| 0.07 | 77.62 | 0.07 | 273.96 |
| 0.08 | 73.02 | 0.08 | 267.85 |
| 0.09 | 68.63 | 0.09 | 262.29 |
| 0.1 | 64.49 | 0.1 | 25719 |

Table 2 summarizes best-fit parameters obtained by non-linear curve fitting analysis, as well as the average percentage error (Eq. 3). The Freundlich exponent varies between 0.23 and 0.43, which indicates favourable adsorption for chlorobenzene ($0 < n < 1$). k_F values are relatively low, especially at the lowest temperature of 283 K, which corresponds to sites of weak activity. Values of Langmuir monolayer capacity (q_{mL}) and Freundlich constant (k_F) increase with temperature, evidencing the endothermic nature of the adsorption process. The influence of temperature increases as particle size is increased, while the increase in Freundlich constant n with temperature can be explained by an increase in the heterogeneity of available sites for adsorption.

The Redlich-Peterson model was found to fit the experimental data with the highest accuracy (minimum mean APE) and was, therefore, chosen as the most suitable one. This model can be applied in a wide range of CB concentrations. Redlich-Peterson fits are depicted in Fig. 3, which shows the superposition of experimental results (points) and the theoretical calculated data (lines). The Redlich-Peterson equation has several properties which make it suitable for being used in many adsorption systems. At low surface coverage it is reduced to a linear isotherm. At high concentrations of adsorbate it becomes the Freundlich isotherm, and for the special case of $\beta = 0$ it becomes the Langmuir isotherm. Data showed in evidence that for particle sizes ranging from

0.50 to 1.68 mm, the values of β increase with temperature whereas for the smallest particle size the opposite trend is observed.

C. Thermodynamic study

Apparent isosteric heat of adsorption ($\Delta H_{st,a}$) at constant surface coverage q (g/g) for CB was calculated using the Clausius-Clapeyron equation (Chang, 1998):

$$\frac{d \ln C_e}{dT} = \frac{\Delta H_{st,a}}{RT^2} \quad (9)$$

where R is the ideal gas constant, C_e (g/L) is the equilibrium concentration at T (K), and $\Delta H_{st,a}$ is the apparent isosteric heat of adsorption (kJ/mol). For q constant,

$$\Delta H_{st,a} = \left. \frac{Rd \ln C_e}{dT} \right]_{-q_e} \quad (10)$$

For obtaining $\Delta H_{st,a}$, the equilibrium concentration (C_e) at constant amount of adsorbate was obtained from the adsorption isotherm data, and $\Delta H_{st,a}$ was calculated from the slope of the $\ln C_e$ versus $(1/T)$ plot for different amounts chlorobenzene onto GAC. Table 3 shows the calculated isosteric enthalpies $\Delta H_{st,a}$ values at different surface coverages as obtained from Eq. (10). The apparent isosteric heat of adsorption in aqueous solutions, $\Delta H_{st,a}$, is the resultant of the net isosteric heat of adsorption $\Delta H_{st,net}$ and the heat of solution ΔH_{sol} of the adsorbate in the solvent. Standard heat of solution of chlorobenzene in methanol is 0.71 kJ/mol (Korolev *et al.*, 2007), which will be next to standard heat of solution of chlorobenzene in water, because of chlorobenzene do not contain terminal OH groups and is unable to donate protons without rupture of the alcohol hydrogen bonds. So, $\Delta H_{st,net}$ value should be almost equal to $\Delta H_{st,a}$ and it will be used in the following analysis for both low temperature and high temperatures ranges.

It was found that the isosteric heat of adsorption of CB onto GAC was a function of surface coverage. Fig. 4 evidences that the heat of adsorption decreases with the amount of CB adsorbed. This is a consequence of the heterogeneous nature of the adsorbent surface, to-

gether with the preferential occupation of the energetically more favorable active sites. The positive sign reveals it is an endothermic process, with values ranging between 65–288 kJ/mol, which are within the typical range of chemical adsorption.

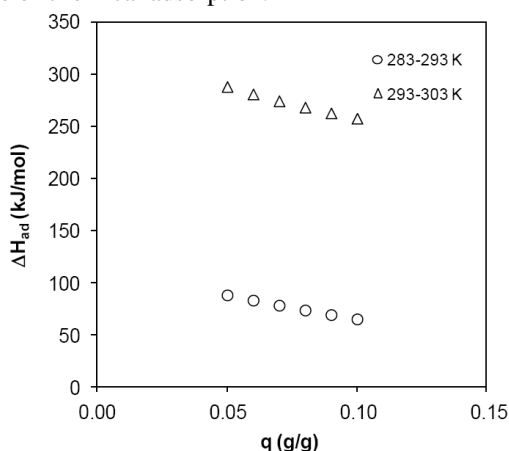


Figure 4. Dependence of the heat of adsorption with the amount of solute adsorbed.

This endothermic nature is opposite to the effect of temperature on the chemical adsorption of a single component (e.g., a gas on a solid), because adsorption from solution involves at least two components, a solute and solvent. Adsorption from solution is influenced not only by adsorbent–adsorbate interactions but also adsorbate–solvent and adsorbent–solvent interactions (Corkill *et al.*, 1966).

The isosteric heat of adsorption increases with temperature. This behavior may be due to the existence of a kinetic energy barrier in the overall adsorption process. Above a certain temperature it could be expected a change of this trend. An temperature increase weakens the hydrogen bonds formed among water molecules and between water molecules and solute or adsorbent (Terzyk, 2004), thus increases diffusion in pores (Iriarte-Velasco *et al.*, 2011). Consequently, a temperature increase promotes dehydration adsorption of molecules CB, making them flat and there is an increase of its dipole moment. The increase in planarity gives CB molecules greater accessibility to the microporosity of the AC, while the increase in dipolar moment results in enhanced adsorbent–adsorbate interactions. As a result of this process, CB adsorption could be apparently endothermic.

Furthermore, the value of $q_{mL} \cdot k_L$, being q_{mL} the monolayer capacity and k_L the Langmuir constant, is related to adsorbate–adsorbent interactions. The value of $q_{mL} \cdot k_L$ decreased from 35.9 at 283 K to 29.1 at 303 K (particle size 0.5 to 0.70 mm), indicating that these interactions decreased with temperature. This is in good agreement with the rise in the absolute values of heat of adsorption (endothermic) observed in this study.

IV. CONCLUSIONS

The adsorption of chlorobenzene onto GAC of different particle size was studied at temperatures from 283 to 303 K. The experimental kinetic values were suitably

fitted to a hyperbolic expression, which corresponds to the pseudo-second-order kinetic model, as well as to the intraparticle diffusion model. The intraparticle diffusion was the rate controlling step, and the initial concentration of CB was the most significant parameter affecting mass transfer coefficient.

Equilibrium data were fitted to Langmuir, Freundlich and Redlich-Peterson models. The latter was the most suitable one, given that it provides the best fitting in a wide range of adsorption conditions. The equilibrium uptake capacity increased with temperature, evidencing the endothermic nature of this adsorption system. The apparent isosteric heat of adsorption varied in the range between 65–288 kJ/mol, which is within the typical range of chemical adsorption. The absolute value of the isosteric heat of adsorption decreased with surface coverage and increased with adsorption temperature. The first trend can be explained by the heterogeneous nature of the adsorbent surface, together with the preferential occupation of the energetically more favorable active sites. The second one is representative of a weakening of adsorbate–solvent and adsorbent–solvent interactions with temperature. The influence of adsorption temperature is a relevant issue, since adsorption temperatures may significantly vary depending on the source of wastewater.

REFERENCES

- Ahmed, M.N. and R.N. Ram, "Removal of Basic Dye from Waste-Water Using Silica as Adsorbent," *Environmental Pollution*, **77**, 79-86 (1992).
- Chang, R., *Chemistry*, McGraw-Hill, Boston (1998).
- Chowdhury P. and T. Viraraghavan, "Sonochemical degradation of chlorinated organic compounds, phenolic compounds and organic dyes - A review," *Science of the Total Environment*, **407**, 2474-2492 (2009).
- Corkill, J.M., J.F. Goodman and J.R. Tate, "Adsorption of Non-Ionic Surface-Active Agents at Graphon/Solution Interface," *Transactions of the Faraday Society*, **62**, 979-986 (1966).
- Cotoruelo, L.M., M.D. Marques, J. Rodriguez-Mirasol, J.J. Rodriguez and T. Cordero, "Lignin-based activated carbons for adsorption of sodium dodecylbenzene sulfonate: Equilibrium and kinetic studies," *Journal of Colloid and Interface Science*, **332**, 39-45 (2009).
- Cotoruelo, L.M., M.D. Marques, F.J. Diaz, J. Rodriguez-Mirasol, J.J. Rodriguez and T. Cordero, "Equilibrium and Kinetic Study of Congo Red Adsorption onto Lignin-Based Activated Carbons," *Transport in Porous Media*, **83**, 573-590 (2010).
- Croue, J.P., D. Violleau, C. Bodaire and B. Legube, "Removal of hydrophobic and hydrophilic constituents by anion exchange resin," *Water Science and Technology*, **40**, 207-214 (1999).
- Environment Protection Agency, U.S. EPA/600/8-84/015F. Office of Health and Environmental Assessment, Washington, DC. (1985).

- Gusler, G.M., T.E. Browne and Y. Cohen, "Sorption of Organics from Aqueous-Solution Onto Polymeric Resins," *Industrial & Engineering Chemistry Research*, **32**, 2727-2735 (1993).
- Iriarte-Velasco, U., N. Chimeno-Alanis, M.P. Gonzalez-Marcos and J.I. Alvarez-Uriarte, "Relationship between Thermodynamic Data and Adsorption/Desorption Performance of Acid and Basic Dyes onto Activated Carbons," *Journal of Chemical and Engineering Data*, **56**, 2100-2109 (2011).
- Korolev, V.P., Y.A. Kasina and N.L. Smirnova, "Comparative study of benzene, chlorobenzene, and aniline solvation by alcohol-alcohol and alcohol-alkane mixtures," *Russian Journal of General Chemistry*, **77**, 1708-1714 (2007).
- Lin, M.L., Z.W. Zhao, F.Y. Cui and S.J. Xia, "Modeling of equilibrium and kinetics of chlorobenzene (CB) adsorption onto powdered activated carbon (PAC) for drinking water treatment," *Desalination and Water Treatment*, **44**, 245-254 (2012).
- Liu, Y., "New insights into pseudo-second-order kinetic equation for adsorption," *Colloids and Surfaces A-Physicochemical and Engineering Aspects*, **320**, 275-278 (2008).
- Real Decreto, 140/2003 de 7 de febrero por el que se establecen los criterios sanitarios de la calidad del agua de consumo humano/BOE 21-2-2003, Madrid (2003).
- Redlich, O. and D.L. Peterson, "A new adsorption isotherm," *J. Phys. Chem.*, **63**, 1024-1026 (1959).
- Sennour, R., G. Mimane, A. Benghalem and S. Taleb, "Removal of the persistent pollutant chlorobenzene by adsorption onto activated montmorillonite," *Applied Clay Science*, **43**, 503-506 (2009).
- Terzyk, A.P., "The effect of carbon surface chemical composition on the adsorption of acetanilide," *Journal of Colloid and Interface Science*, **272**, 59-75 (2004).
- Tsai, W.T., C.Y. Chang, S.Y. Wang, C.F. Chang, S.F. Chien and H.F. Sun, "Cleaner production of carbon adsorbents by utilizing agricultural waste corn cob," *Resources Conservation and Recycling*, **32**, 43-53 (2001).
- van den Heuvel, H. and P.C.M. van Noort, "Removal of indigenous compounds to determine maximum capacities for adsorption of phenanthrene by sediments," *Chemosphere*, **54**, 763-769 (2004).
- Walker, G.M., L. Hansen, J.A. Hanna and S.J. Allen, "Kinetics of a reactive dye adsorption onto dolomitic sorbents," *Water Research*, **37**, 2081-2089 (2003).
- Wang, Y. and H.K. Lee, "Determination of chlorobenzenes in water by solid-phase extraction and gas chromatography mass spectrometry," *Journal of Chromatography A*, **803**, 219-225 (1998).
- Yapar, S., V. Ozbudak, A. Dias and A. Lopes, "Effect of adsorbent concentration to the adsorption of phenol on hexadecyl trimethyl ammonium-bentonite," *Journal of Hazardous Materials*, **121**, 135-139 (2005).
- Zhu, L.L., Y.F. Deng, J.P. Zhang and J. Chen, "Adsorption of phenol from water by N-butylimidazolium functionalized strongly basic anion exchange resin," *Journal of Colloid and Interface Science*, **364**, 462-468 (2011).

Received: March 30, 2013

Accepted: August 21, 2013

Recommended by Subject Editor: María Luján Ferreira